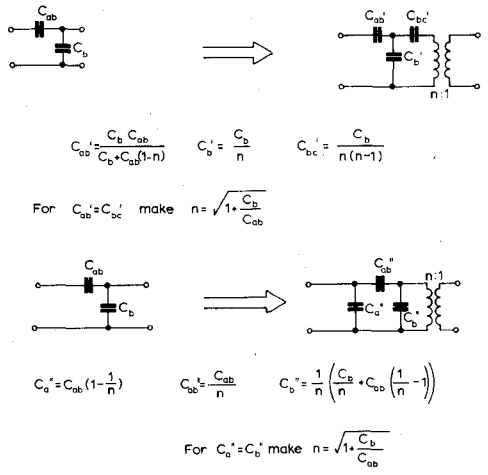

ACKNOWLEDGMENT

The author wishes to extend his thanks and appreciation to B. Hoad and R. S. Watts for their skilled assistance in the construction of laboratory models.

REFERENCES

[1] P. I. Richards, "Resistor-transmission line circuits," *Proc. IRE*, vol. 36, pp. 217–220, Feb. 1948.

[2] M. C. Horton and R. J. Wenzel, "General theory and design of optimum quarter-wave TEM filters," *IEEE Trans. Microwave Theory Tech.*, vol. MTT-13, pp. 316–327, May 1965.

[3] H. J. Orchard and G. C. Temes, "Filter design using transformed variables," *IEEE Trans. Circuit Theory*, vol. CT-15, pp. 385–408, Dec. 1968.

[4] R. J. Wenzel, "Synthesis of combline and capacitively loaded interdigital bandpass filters of arbitrary bandwidth," *IEEE Trans. Microwave Theory Tech.*, vol. MTT-19, pp. 678–686, Aug. 1971.

[5] S. B. Cohn, "Characteristic impedance of shielded strip transmission line," *IRE Trans. Microwave Theory Tech.*, vol. MTT-2, pp. 52–55, July 1954.

[6] S. B. Cohn, "Shielded coupled-strip transmission line," *IRE Trans. Microwave Theory Tech.*, vol. MTT-3, pp. 29–38, Oct. 1955.

[7] S. B. Cohn, "Thickness corrections for capacitive obstacles and strip conductors," *IRE Trans. Microwave Theory Tech.*, vol. MTT-8, pp. 638–644, Nov. 1960.

[8] G. L. Matthaie, L. Young, and E. M. T. Jones. *Microwave Filters, Impedance-Matching Networks and Coupling Structures.* New York: McGraw-Hill, 1964.

✤

Brian J. Minnis was born in Sheffield, England, in 1953. He received the B.Sc. (honors) degree in electronics from the University of Kent at Canterbury in 1973.

After graduating, he joined MEL at Crawley and worked on the design of various microwave components. At the end of 1974 he took up a post as Lecturer in Telecommunications at a college of further education in Hertfordshire. In 1976 he joined Marconi Space and Defence Systems at Stanmore and worked on the design of microwave antennas and radomes. Since 1978 he has been working at Philips Research Laboratories where his main field of interest has been broadband microwave filter design.

On Design and Performance of Lossy Match GaAs MESFET Amplifiers

KARL B. NICLAS, SENIOR MEMBER, IEEE

Abstract—**The noise figure, the gain, and the reflection coefficients of lossy match amplifiers and their dependence on circuit elements are studied. Theoretical results are supported by measured data taken on a two-stage unit. In addition, the performance characteristics of a 100–8800 MHz four-stage lossy match amplifier are discussed. The unit exhibits 23.3 ± 1.1 dB of gain over the nearly 6-1/2 octaves. Its maximum noise figure is 10.9 dB from 100–8800 MHz and 6.6 dB from 2000–8000 MHz. The amplifier's overall circuit dimensions are 10 × 5.7 mm.**

I. INTRODUCTION

THE BALANCED amplifier concept has dominated solid-state amplifier design for nearly two decades [1]. While it is expected to continue its dominating role, it will not go unchallenged by three single-ended amplifier concepts that have made great progress in the field of broadband amplification over the last few years. These three principles, which are presently competing for the best single-ended amplifier performance, are [2]–[7] 1) the matched feedback amplifier; 2) the lossy match amplifier; and 3) the distributed amplifier. They all are characterized by their compact size and, at least the first two by their simplicity and low cost. It is for these reasons that the matched single-ended amplifier concepts are very attractive whenever an economical solution to wide-band amplification is of primary concern.

The application of dissipative gain compensation in interstage matching networks [8] and amplifier stabilization by means of resistive-loaded shunt networks [9] have been

Manuscript received March 26, 1982; revised May 11, 1982.

The author is with the Watkins–Johnson Company, 3333 Hillview Avenue, Palo Alto, CA 94304.

0018-9480/82/1100-1900$00.75 ©1982 IEEE

known for many years. Very recently analytic design techniques for an amplifier output network have been proposed [10]. It is the purpose of this paper to provide a better understanding of the electrical behavior of lossy match amplifiers and to study the influence of the individual circuit elements on the amplifier's performance characteristics such as noise figure, gain, and reflection coefficients. Formulas that express the important tradeoffs that exist between gain and reflection coefficients have been developed and are discussed. Furthermore, formulas for the amplifier's noise figure and minimum noise figure are presented. Finally, the experimental and theoretical results of a two-stage lossy match amplifier are compared and the measured performance of a compact ultrawide-band four-stage amplifier is reviewed.

II. Study of Performance Parameters

A. Gain and Reflection Coefficients

The electrical behavior of an amplifier at microwave frequencies is best described by its scattering parameters which are a measure of the unit's insertion gain ($|S_{21}|^2$), its input and output reflection coefficients (S_{11} and S_{22}), as well as its reverse isolation ($|S_{12}|^2$).

The schematic of a multistage lossy match amplifier as it is used in our experiments is shown in Fig. 1. This amplifier can be divided into three basic circuit functions: input matching, amplification, and interstage matching. The topology of the basic lossy match amplifier block containing dissipative circuit elements across its input and output terminals may be represented by the diagram shown in Fig. 2(a). The two-port between these two resistive shunt elements consists of the transistor and any additional elements that may be required for a desired performance. In the case of the basic amplifier block in Fig. 3(a), an open circuit shunt stub cascaded with a 90-Ω transmission line at the transistor's drain terminal serves such a purpose.

Using the admittance representation of Fig. 2(a), one can easily derive the scattering parameters of this network. The results are presented as (A1) in the Appendix. Additional algebraic steps lead to an important relationship between S_{21} and the reflection coefficients S_{11} and S_{22} of the basic amplifier block

$$S_{21} = -\frac{Y_0}{Y_{12}}\left[\sqrt{1+\frac{Y_{21}Y_{12}}{Y_0^2}(1+S_{11})(1+S_{22})}-1\right]. \quad (1)$$

This expression leads to the calculation of the impact of any improvement of the reflection coefficients

$$S_{11} = \frac{[Y_0-(Y_{11}+Y_G)][Y_0+(Y_{22}+Y_D)]+Y_{12}Y_{21}}{[Y_0+(Y_{11}+Y_G)][Y_0+(Y_{22}+Y_D)]-Y_{12}Y_{21}} \quad (2a)$$

$$S_{22} = \frac{[Y_0+(Y_{11}+Y_G)][Y_0-(Y_{22}+Y_D)]+Y_{12}Y_{21}}{[Y_0+(Y_{11}+Y_G)][Y_0+(Y_{22}+Y_D)]-Y_{12}Y_{21}} \quad (2b)$$

(Y_0—characteristic admittance)

by means of the admittances Y_G and Y_D on the unit's gain $|S_{21}|^2$.

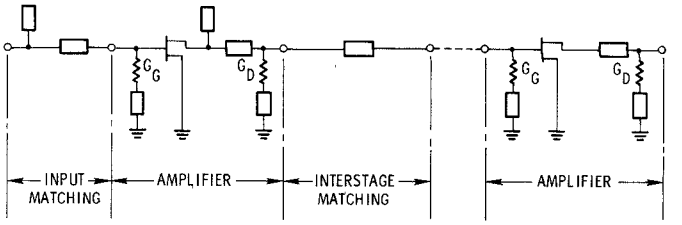

Fig. 1. Circuit topology of a multistage lossy match amplifier.

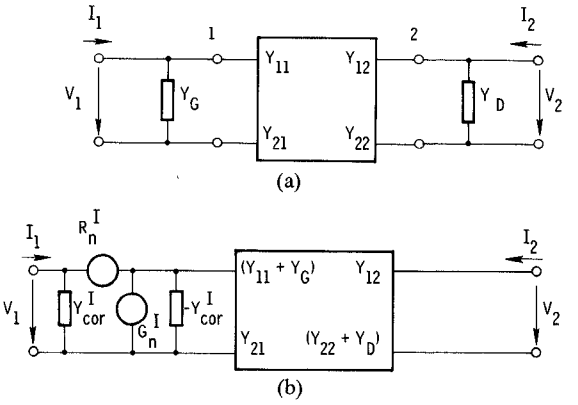

Fig. 2. Block diagram of the basic lossy match amplifier for the determination of (a) the scattering parameters and (b) the equivalent noise parameters.

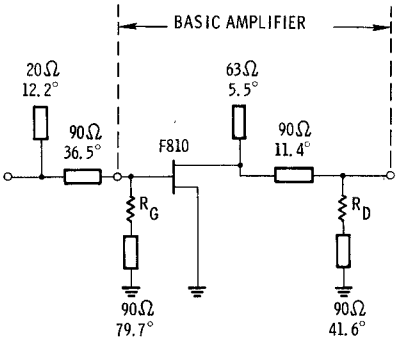

(a)

Equivalent Circuit Elements of WJ-F 810

g_m = 57 mS	R_g = 2.0 ohms
τ_0 = 4 p sec	L_g = .208 nH
C_{gs} = .508 pF	R_s = 1.0 ohms
C_{gd} = .041 pF	L_s = .169 nH
C_{dc} = .035 pF	C_{ds} = .136 pF
R_{gs} = 5.6 ohms	R_d = 2 ohms
R_{ds} = 257 ohms	L_d = .146 nH

(b)

Fig. 3. Circuit topology of (a) a single-stage lossy match amplifier and (b) equivalent circuit elements of the GaAs MESFET.

In many practical cases the condition

$$\left|\frac{Y_{21}Y_{12}}{Y_0^2}(1+S_{11})(1+S_{22})\right| \ll 1 \quad (3)$$

is satisfied and (1) adopts the much simpler form

$$S_{21} \simeq -\frac{Y_{21}}{2Y_0}(1+S_{11})(1+S_{22}). \tag{4}$$

A close examination of (2) reveals that the input and output reflection coefficients S_{11} and S_{22} can only be made zero by means of the lossy shunt elements Y_G and Y_D as long as

$$G_{\text{in}} \leqslant Y_0 \tag{5a}$$

$$G_{\text{out}} \leqslant Y_0 \tag{5b}$$

where G_{in} and G_{out} are the conductances of the input and output admittances

$$Y_{\text{in}} = G_{\text{in}} + jB_{\text{in}} = Y_{11} + Y_G - \frac{Y_{12}Y_{21}}{Y_0 + Y_{22} + Y_D} \tag{6a}$$

$$Y_{\text{out}} = G_{\text{out}} + jB_{\text{out}} = Y_{22} + Y_D - \frac{Y_{12}Y_{21}}{Y_0 + Y_{11} + Y_G}. \tag{6b}$$

However, even if conditions (5) are not met, input and output matches may be improved by the reactive components of Y_G and Y_D.

In most practical cases of lossy match GaAs MESFET amplifiers, (5) is satisfied over most or at least over the lower portion of the frequency band. In order to improve the matches over the upper portion of the band, conventional matching techniques may be added by employing transmission line elements and open-circuit shunt stubs outside of the basic lossy match amplifier of Fig. 2(a). This may be accomplished in form of the input and interstage matching networks shown in Fig. 1.

The insertion gain of the basic amplifier derived from (2) is

$$\text{Gain} = \left|\frac{Y_0}{Y_{12}}\right|^2 \left|\sqrt{1+\frac{Y_{21}Y_{12}}{Y_0^2}(1+S_{11})(1+S_{22})} - 1\right|^2. \tag{7}$$

At frequencies where (3) is satisfied, the exact formula for gain (7) can be replaced by

$$\text{Gain} \simeq \frac{1}{4}\left|\frac{Y_{21}}{Y_0}\right|^2 |1+S_{11}|^2 |1+S_{22}|^2. \tag{8}$$

The error when using (8) in case of the basic amplifier contained in Fig. 3(a) for $R_G = R_D = 100\ \Omega$ does not exceed 0.25 dB up to frequencies of 5 GHz.

While (7) expresses the tradeoffs between gain and reflection coefficients in its exact form, they can most easily be demonstrated on the basic amplifier's low-frequency model. For frequencies up to 1 GHz, the reactive elements of the transistor model listed in Fig. 3(b) have relatively little influence on the magnitude of the amplifier's gain and reflection coefficients. As a result, the transistor can be represented by its low-frequency model and the amplifier circuit can be reduced to the simple network inserted in Fig. 4. For this idealized model, the scattering parameters are easily determined. They are

$$S_{11} = \frac{1-G_GZ_0}{1+G_GZ_0} \tag{9a}$$

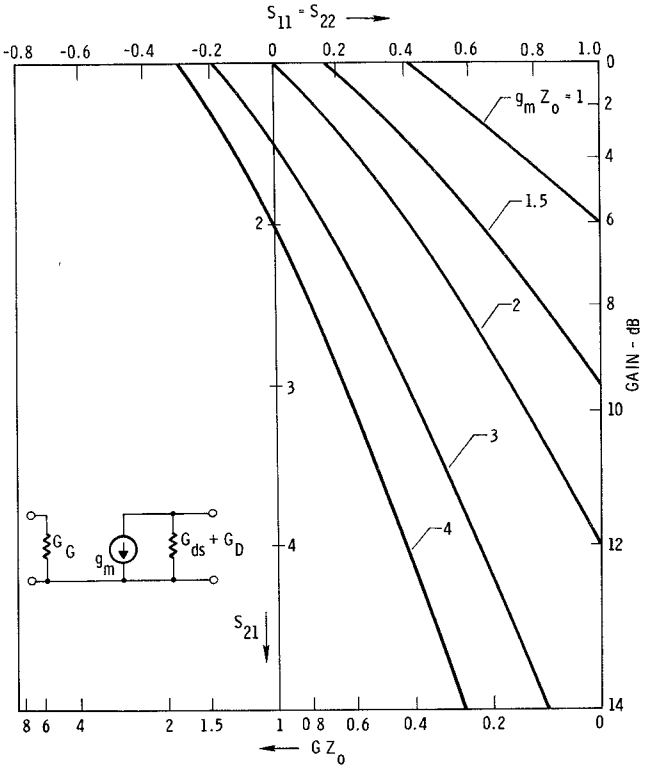

Fig. 4. Gain and reflection coefficients of a symmetric module ($S_{11} = S_{22}$) at low frequencies as a function of $GZ_0 = G_GZ_0 = (G_{ds} + G_D)Z_0$.

and

$$S_{12} = 0 \tag{9b}$$

$$S_{21} = \frac{-2\,g_mZ_0}{[1+G_GZ_0][1+(G_{ds}+G_D)Z_0]} \tag{9c}$$

$$S_{22} = \frac{1-(G_{ds}+G_D)Z_0}{1+(G_{ds}+G_D)Z_0}$$

(Z_0—characteristic impedance). (9d)

Furthermore, substituting $Y_{21} = g_m$ and $Y_{12} = 0$ into (1), where g_m is the transconductance, results in

$$S_{21} = -\frac{g_mZ_0}{2}(1+S_{11})(1+S_{22}). \tag{10}$$

At low frequencies, S_{11} and S_{22} have negligible imaginary components, and the gain can be expressed as

$$\text{Gain} = |S_{21}|^2 = \left[\frac{g_mZ_0}{2}(1+S_{11})(1+S_{22})\right]^2 \tag{11}$$

which clearly expresses the tradeoffs between the gain and the reflection coefficients. This relationship is presented in graphical form in Fig. 4 for a lossy match amplifier with identical input and output conductances; i.e., $G_G = G_{ds} + G_D = G$, resulting in $S_{11} = S_{22}$.

B. *Noise Parameters and Noise Figure*

The exact noise parameters of the basic lossy match amplifier [11] shown in Fig. 2(a) are

$$R_n^I = R_n + \frac{G_D}{|Y_{21}|^2} \tag{12a}$$

and

$$G_n^I = G_n + G_G + |Y_{11} - Y_{\text{cor}}|^2 \frac{G_D R_n}{|Y_{21}|^2 R_n + G_D} \quad (12b)$$

$$Y_{\text{cor}}^I = Y_{\text{cor}} + Y_G + (Y_{11} - Y_{\text{cor}}) \frac{G_D}{|Y_{21}|^2 R_n + G_D}. \quad (12c)$$

Their elements are located outside of the "noiseless" two-port as shown in Fig. 2(b). R_n, G_n, and Y_{cor} are the equivalent noise resistance, equivalent noise conductance, and the correlation admittance, respectively of the two-port in Fig. 2(a) embedded between the shunt admittances Y_G and Y_D.

The exact minimum noise figure of our lossy match amplifier can now be calculated with

$$F_{\min}^I = 1 + 2\left[R_n^I G_{\text{cor}}^I + \sqrt{R_n^I G_n^I + \left(R_n^I G_{\text{cor}}^I\right)^2} \right]. \quad (13)$$

Fortunately, a number of conditions can be formulated that are satisfied in most cases of practical lossy match amplifier design and significantly simplify the resulting formula for the minimum noise figure. A condition met with few exceptions is

$$G_D \ll |Y_{21}|^2 R_n. \quad (14a)$$

If, in addition to (14a)

$$|Y_{11} - Y_{\text{cor}}|^2 G_D \ll |Y_{21}|^2 (G_n + G_G) \quad (14b)$$

and

$$G_{11} G_D \ll |Y_{21}|^2 R_n (G_{\text{cor}} + G_G) \quad (14c)$$

the minimum noise figure (13) may be expressed in the form

$$F_{\min}^I \simeq 1 + 2R_n \left[(G_{\text{cor}} + G_G) + \sqrt{\frac{(G_n + G_G)}{R_n} + (G_{\text{cor}} + G_G)^2} \right]. \quad (15)$$

Under the same conditions (14), the amplifier's noise figure [12], [13] is

$$F^I \simeq F_{\min}^I + \frac{R_n}{G_s^I}\left(G_s^I - G_{s\min}^I\right)^2 + \frac{R_n}{G_s^I}\left(B_s^I - B_{s\min}^I\right)^2 \quad (16)$$

with the source admittance

$$Y_s^I = G_s^I + jB_s^I \quad (16a)$$

and the source admittance for the minimum noise figure

$$Y_{s\min}^I = G_{s\min}^I + jB_{s\min}^I \simeq \sqrt{\frac{G_n + G_G}{R_n} + (G_{\text{cor}} + G_G)^2} - j\left(B_{\text{cor}} + B_G + B_{11} \frac{G_D}{|Y_{21}|^2 R_n} \right). \quad (16b)$$

III. Amplifier Design

As is the case for all broad-band microwave solid-state amplifiers, the lossy match amplifier's performance improves with increasing transconductance and decreasing

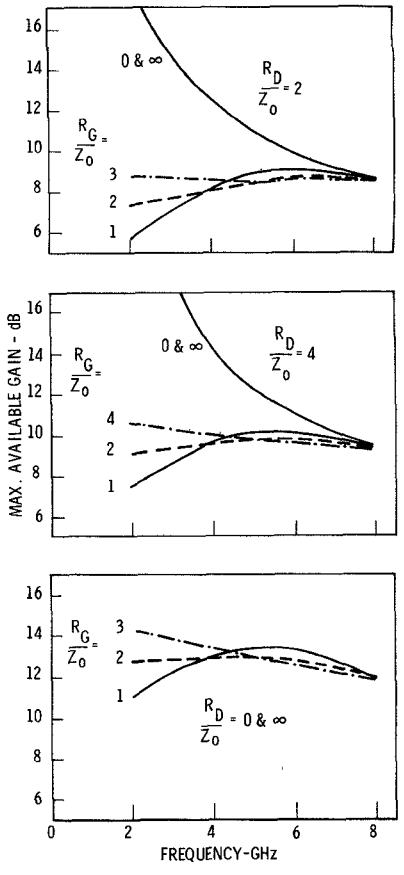

Fig. 5. The maximum available gain of the amplifier module (Fig. 3(a)) versus frequency with R_G/Z_0 and R_D/Z_0 as parameters.

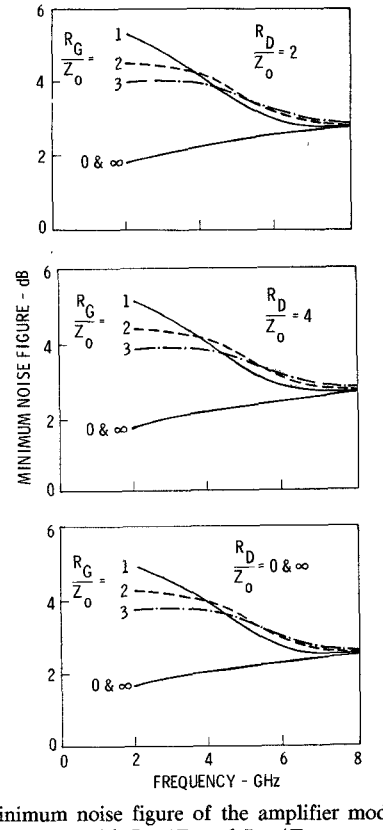

Fig. 6. The minimum noise figure of the amplifier module (Fig. 3(a)) versus frequency with R_G/Z_0 and R_D/Z_0 as parameters.

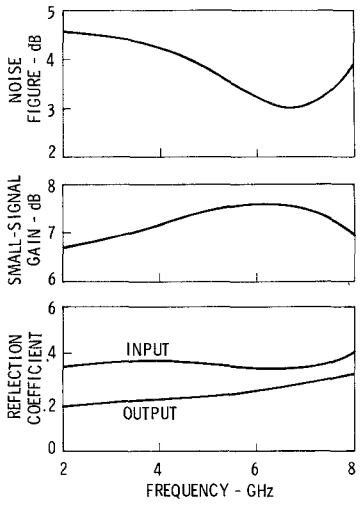

Fig. 7. Noise figure, gain, and reflection coefficients of the amplifier module (Fig. 3(a)) versus frequency with $R_G = R_D = 100\ \Omega$.

parasitics of the GaAs MESFET. The normalized transconductance of the transistor as demonstrated by the curves in Fig. 4 should be $g_m Z_0 = 2$ or greater in order to obtain reasonable gains and acceptable reflection coefficients. It is irrelevant whether high transconductance is achieved by one GaAs MESFET or several that are paralleled as long as parasitics don't limit the amplifier's performance at the high end of the desired frequency band.

The GaAs MESFET used in our experiments is the WJ-F810 whose equivalent circuit elements are listed in Fig. 3(b) and whose equivalent noise parameters have been published and discussed elsewhere [14]. The F810 has a normalized transconductance of $g_m Z_0 = 2.85$. Choosing $G = G_G = G_{ds} + G_D = 10$ mS, one finds the gain and the reflection coefficients from Fig. 4: $G = 8.1$ dB and $S_{11} = S_{22} = 0.33$. Taking into account that $R_{ds} = 257\ \Omega$, the corresponding resistances are $R_G = 100\ \Omega$ and $R_D = 164\ \Omega$. Since the drain current I_{ds} of the transistor flows through R_D it causes a significant voltage drop. In order to reduce this voltage drop and to simultaneously create better interstage matching conditions, it is advisable to reduce R_D. Using (9) and (11) one calculates $G = 7.0$ dB, $S_{11} = 0.33$, and $S_{22} = 0.18$ for $R_G = R_D = 100\ \Omega$. Since gain decreases rapidly with frequency the resistive loss needs to be gradually reduced with frequency which is accomplished by the short-circuit shunt stubs in series with the resistors R_G and R_D of the circuit in Fig. 3(a). One finds that the electrical lengths of these high impedance lines is significantly less critical on the drain side of the amplifier. Introduction of the short-circuit shunt stubs significantly increases the gain over the second half of the frequency band and gain experiences a further improvement by placing the two circuit elements (see Fig. 3(a)) between the drain terminal and the resistive-loaded shunt circuit. Finally, the input reflection coefficient is reduced over the entire band by means of the simple input matching network shown in Fig. 3(a).

In order to demonstrate the influence of the resistors R_G and R_D on the module's optimum performance, the computed maximum available gain and minimum noise figure are plotted in Figs. 5 and 6, respectively. A comparison of the curves in Fig. 6 clearly illustrates that R_D has hardly any influence on the minimum noise figure of the amplifier module as one might expect for

$$\frac{G_D}{|Y_{21}|^2 R_n} \leqslant 0.22$$

across the 2–8-GHz band. The computed noise figure, gain, and reflection coefficients for $R_G = R_D = 100\ \Omega$ are plotted in Fig. 7.

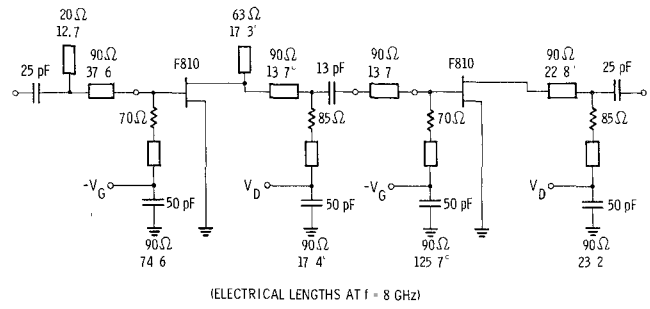

Fig. 8. Circuit topology of the computer optimized two-stage amplifier with the shunt resistors $R_G = 70\ \Omega$ and $R_D = 85\ \Omega$.

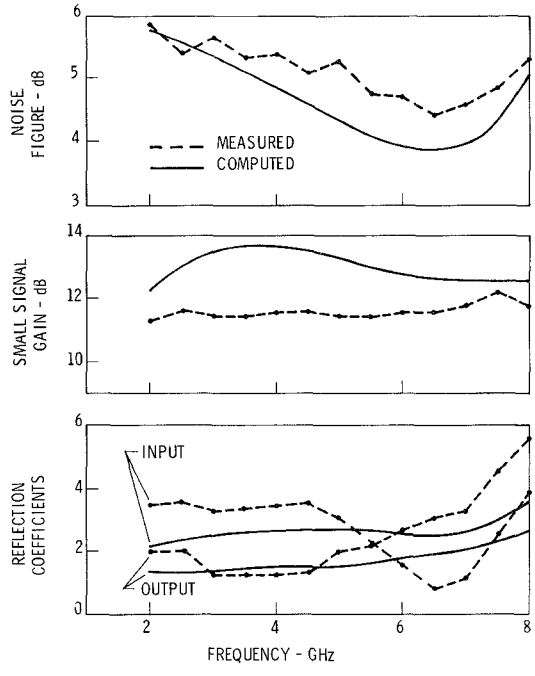

Fig. 9. Comparison of the computed and the measured performance characteristics of the two-stage amplifier of Fig. 8.

IV. Performance of Practical Amplifiers

When cascading lossy match amplifier modules, some of the unit's circuit elements require values somewhat different from those of the schematic in Fig. 3(a). This is due to the fact that the inputs and outputs of individual stages are no longer terminated by 50-Ω impedances.

The topology of a computer optimized two-stage amplifier is given in Fig. 8. The lossy match resistors $R_G = 70\ \Omega$ and $R_D = 85\ \Omega$ were not subjected to the optimization routine but rather determined experimentally by trying to

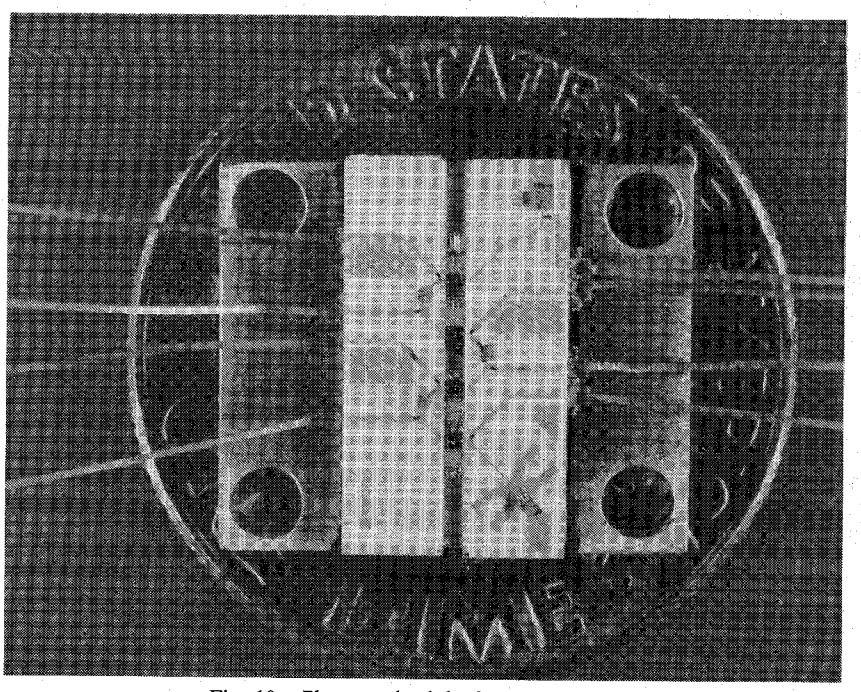

Fig. 10. Photograph of the four-stage amplifier.

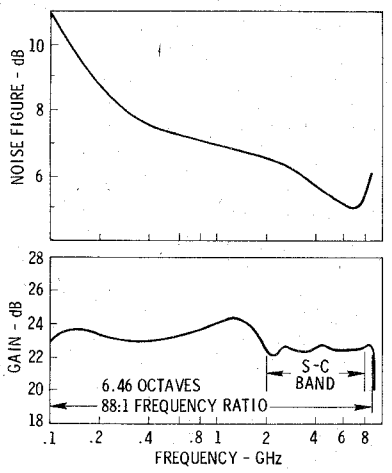

Fig. 11. Measured gain and noise figure of the four-stage amplifier.

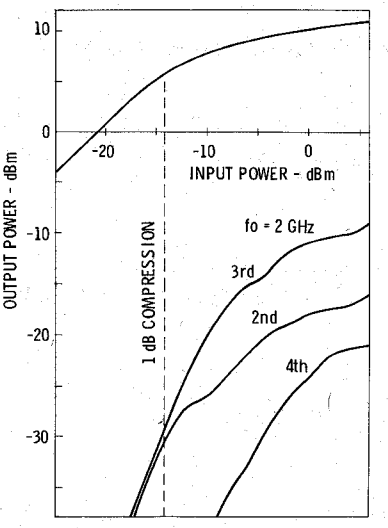

Fig. 12. Fundamental and harmonic output power of a four-stage amplifier ($V_{DS} = 4$ V, $I_{DS} = 35$ mA each).

achieve flat gain performance over the 2–8-GHz band. The measured and computed noise figures, gains, and reflection coefficients for this two-stage amplifier are compared in Fig. 9.

Increasing the number of stages from two to four and attempting to achieve flat gain performance required an additional reduction in the lossy match resistances to $R_G = 60\ \Omega$ and $R_D = 80\ \Omega$. In addition, an increase in the impedances of the amplifier's transmission line elements from 90 Ω to 115 Ω became necessary. A photograph of this amplifier is shown in Fig. 10. Realized on 0.025 in alumina, the overall circuit length of the unit is 0.394 in. or 10 mm. The unique layout of the circuit limits the number of substrates to two regardless of the number of stages and allows the transistors to be die attached to a single cooling rib. Measured gain and noise figures of this amplifier are plotted in Fig. 11. The results demonstrate the enormous bandwidth capacity of the lossy match principle. Extending the band to still lower frequencies is merely a question of using higher value bias and blocking capacitors. The output versus input curves of fundamental and harmonic output power of an earlier four-stage unit for $f_0 = 2$ GHz are plotted in Fig. 12 when operating each transistor at 4 V of drain–source voltage and 35 mA of drain–source current.

V. Conclusion

The noise figure, the gain, and the reflection coefficients of the lossy match amplifier have been studied and formulas to calculate these parameters were developed. Based on the theoretical results a two-stage amplifier was designed and tested. The unit's computed performance was compared with actual test data over the design frequency band of 2–8 GHz. The comparison demonstrates good

agreement between the measured and computed results.

Finally, the measured performance characteristics of a four-stage ultrawide-band amplifier were discussed. This unit has a gain of $G = 23.3 \pm 1.1$ dB and a maximum noise figure of $F = 10.9$ dB over the frequency band of 100–8800 MHz representing nearly 6-1/2 octaves of instantaneous bandwidth. Realized on only two substrates, the overall circuit dimensions are 10.0×5.7 mm with 2.3 dB/mm of gain per unit length. These results evidence the enormous bandwidth potential of the lossy match amplifier achievable in an extremely compact size.

Appendix

The basic circuitry of a lossy match amplifier can be represented by a two-port with lossy elements across its input and output ports as shown in Fig. 2. The two-port between ports 1 and 2 contains the transistor and additional lossless elements that may be required for a desired performance.

The circuit is then characterized by the admittance matrix

$$\begin{bmatrix} I_1 \\ I_2 \end{bmatrix} = \begin{bmatrix} Y_{11} + Y_G & Y_{12} \\ Y_{21} & Y_{22} + Y_D \end{bmatrix} \begin{bmatrix} V_1 \\ V_2 \end{bmatrix} \tag{A1}$$

which can easily be converted into the scattering matrix S_{ij} whose elements are

$$S_{11} = \frac{[Y_0 - (Y_{11} + Y_G)][Y_0 + (Y_{22} + Y_D)] + Y_{12}Y_{21}}{[Y_0 + (Y_{11} + Y_G)][Y_0 + (Y_{22} + Y_D)] - Y_{12}Y_{21}} \tag{A2a}$$

$$S_{12} = \frac{-2Y_{12}Y_0}{[Y_0 + (Y_{11} + Y_G)][Y_0 + (Y_{22} + Y_D)] - Y_{12}Y_{21}} \tag{A2b}$$

$$S_{21} = \frac{-2Y_{21}Y_0}{[Y_0 + (Y_{11} + Y_G)][Y_0 + (Y_{22} + Y_D)] - Y_{12}Y_{21}} \tag{A2c}$$

$$S_{22} = \frac{[Y_0 + (Y_{11} + Y_G)][Y_0 - (Y_{22} + Y_D)] + Y_{12}Y_{21}}{[Y_0 + (Y_{11} + Y_G)][Y_0 + (Y_{22} + Y_D)] - Y_{12}Y_{21}}$$

(Y_0—characteristic admittance). (A2d)

Using the S-parameters of (A2) one obtains

$$S_{21} = \frac{-Y_{21}}{Y_0 + Y_{11} + Y_G}(1 + S_{22}) = \frac{-Y_{21}}{Y_0 + Y_{22} + Y_D}(1 + S_{11}) \tag{A3}$$

suggesting a tradeoff that exists between reflection coefficients and insertion gain. This tradeoff becomes more evident when substituting for $(Y_{11} + Y_G)$ and $(Y_{22} + Y_D)$ obtaining

$$S_{21} = -\frac{Y_{21}}{2Y_0} \frac{(1 + S_{11})(1 + S_{22})}{1 - \frac{S_{12}}{2}\frac{Y_{21}}{Y_0}} \tag{A4}$$

and with

$$S_{21}Y_{12} = S_{12}Y_{21}. \tag{A5}$$

(A4) can finally be expressed as a function of Y_{21} and Y_{12} and the reflection coefficients of the amplifier S_{11} and S_{22}

$$S_{21} = -\frac{Y_0}{Y_{12}}\left[\sqrt{1 + \frac{Y_{21}Y_{12}}{Y_0^2}(1 + S_{11})(1 + S_{22})} - 1\right]. \tag{A6}$$

Acknowledgment

The author would like to thank R. R. Pereira who performed all measurements and the difficult task of tuning the multistage amplifiers. Thanks go also to W. T. Wilser who supervised the fabrication of the GaAs MESFET's and edited the manuscript. The author is indebted to P. Hutchison who typed the complicated formulas.

References

[1] R. S. Engelbrecht and K. Kurokawa, "A wide-band low noise *L*-band balanced transistor amplifier," *Proc. IEEE*, vol. 53, Mar. 1965, pp. 237–247.

[2] E. Ulrich, "Use of negative feedback to slash wideband VSWR," *Microwaves*, pp. 66–70, Oct. 1978.

[3] K. B. Niclas, W. T. Wilser, R. B. Gold, and W. R. Hitchens, "The matched feedback amplifier: Ultrawide-band microwave amplification with GaAs MESFET's," *IEEE Trans., Microwave Theory Tech.*, vol. MTT-28, pp. 285–294, Apr. 1980.

[4] T. Obregon and R. Funk, "A 150-MHz–16-GHz FET amplifier," in *1981 ISSCC, Dig. Tech. Papers*, Feb. 1981.

[5] K. Honjo and Y. Takajama, "GaAs FET ultrabroad-band amplifiers for Gbit/s data rate systems," *IEEE Trans., Microwave Theory Tech.*, vol. MTT-29, pp. 629–636, July 1981.

[6] Y. Ayasli, J. L. Vorhaus, R. L. Mozzi, and L. D. Reynolds, "Monolithic GaAs travelling wave amplifier," *Electron. Lett.*, vol. 17, pp. 413–414, June 11, 1981.

[7] E. W. Strid, K. R. Gleason, and J. Addis, "A dc-12 GHz GaAs FET distributed amplifier," in *1981 Gallium Arsenide Integrated Circuit Symp. Research Abstracts*, p. 47, Oct. 1981.

[8] N. Marshal, "Optimizing multistage amplifiers for low-noise," *Microwaves*, pp. 62–64, Apr. 1974; pp. 60–64, May 1974.

[9] D. P. Hornbuckle and L. J. Kuhlman, Jr, "Broad-band medium-power amplification in the 2–12.4-GHz range with GaAs MESFET's," *IEEE Trans. Microwave Theory Tech.*, vol. MTT-24, pp. 338–342, June 1976.

[10] A. N. Riddle and R. J. Trew, "A broad-band amplifier output network design," *IEEE Trans Microwave Theory Tech.*, vol. MTT-30, pp. 192–196, Feb. 1982.

[11] K. B. Niclas, "The exact noise figure of amplifiers with parallel feedback and lossy matching circuits," *IEEE Trans. Microwave Theory Tech.*, vol. MTT-30, pp. 832–835, May 1982.

[12] H. Rothe and W. Dahlke, "Theory of noisy fourpoles," *Proc. IRE*, vol. 44, pp. 811–818, June 1956.

[13] H. A. Haus, *et al.*, "Representation of noise in linear twoports," *Proc. IRE*, vol. 48, pp. 69–74, Jan. 1960.

[14] K. B. Niclas, "Noise in broad-band GaAs MESFET amplifiers with parallel feedback," *IEEE Trans. Microwave Theory Tech.*, vol. MTT-30, pp. 63–70, Jan. 1982.

Karl B. Niclas (M'63–SM'81) received the Dipl.—Ing. and Doctor of Engineering degrees from the Technical University of Aachen, Aachen, Germany, in 1956 and 1962, respectively.

From 1956 to 1962 he was with the Microwave Tube Laboratory at the Telefunken G.m.b.H. Tube Division, Ulm-Donau, Germany. He was engaged in research and development on ultra-low-noise and medium-power traveling-wave tubes. In 1958 he became Head of the company's

Traveling-Wave Tube Section and Assistant Manager of the Microwave Tube Laboratory. From 1962 to 1963 he was associated as a Senior Project Engineer with General Electric Microwave Laboratory, Stanford, CA. His work was mainly concerned with theoretical and experimental investigations of single-reversal focused low-noise traveling-wave tube amplifiers, and resulted in the first lightweight amplifier of this type. In 1963 he joined the Technical Staff of Watkins–Johnson Company, Palo Alto, CA, and is presently Consultant to the Vice President, Devices Group. His present research efforts are primarily focused on advanced GaAs FET amplifiers, broad-band power combining techniques, and wide-band GaAs FET oscillator concepts. From 1967 to 1976 he was Manager of the company's Tube Division. Before that, he was Head of the Low-Noise Tube R & D Section, and prior to that he was engaged in a research program on new concepts for achieving high efficiency in traveling-wave tubes. He is the author of numerous papers and holds a number of patents.

Dr. Niclas received the outstanding publications award in 1962 of the German Society of Radio Engineers.

Weakly Coupled Dielectric Resonators

JEAN VAN BLADEL, FELLOW, IEEE

Abstract—**The resonant modes of a pair of coupled resonators of high ϵ_r are considered in the limit of large spacings D between resonators. Attention is focused on the lowest "magnetic-moment" mode, where the coupling effect leads to a split of the original mode into an even and an odd part. Formulas are obtained for the coupling coefficient, the resonant frequencies and Q of the modes. They are strikingly similar to those for weakly-coupled $R-L-C$ circuits. The accuracy of the formulas is verified by comparing their predictions with direct numerical data, available for coupled circular cylindrical resonators.**

I. Introduction

THE RESONANT modes of a dielectric resonator of high ϵ_r are obtained by solving the differential problem

$$\begin{aligned} -\operatorname{curl}\operatorname{curl}\bar{h}_m + k_m^2\bar{h}_m = 0 \quad &\text{in the dielectric} \\ \operatorname{curl}\bar{h}_m = 0 \quad &\text{outside the dielectric.} \end{aligned} \tag{1}$$

The eigenvector $\bar{h}_m$ must be continuous across the boundary surface, and of order $1/R^2$ (or higher) at large distances [1]. The numerical solution of (1), a difficult three-dimensional problem, simplifies when the body is of revolution (e.g., a sphere or a circular cylinder [2]). In the coupled structure shown in Fig. 1, (1) must be solved in the presence of a composite dielectric consisting of volumes **1** and **2**. When the spacing between **1** and **2** is small, the field distribution in each volume will be significantly perturbed with respect to that of the resonator isolated in free space. Any simplifying feature, such as symmetry of revolution, will be lost, except in structures of the type shown in Fig. 4.

Manuscript received January 29, 1982; revised May 6, 1982.

The author is with the Laboratory of Electromagnetism and Acoustics, University of Ghent, Ghent, Belgium.

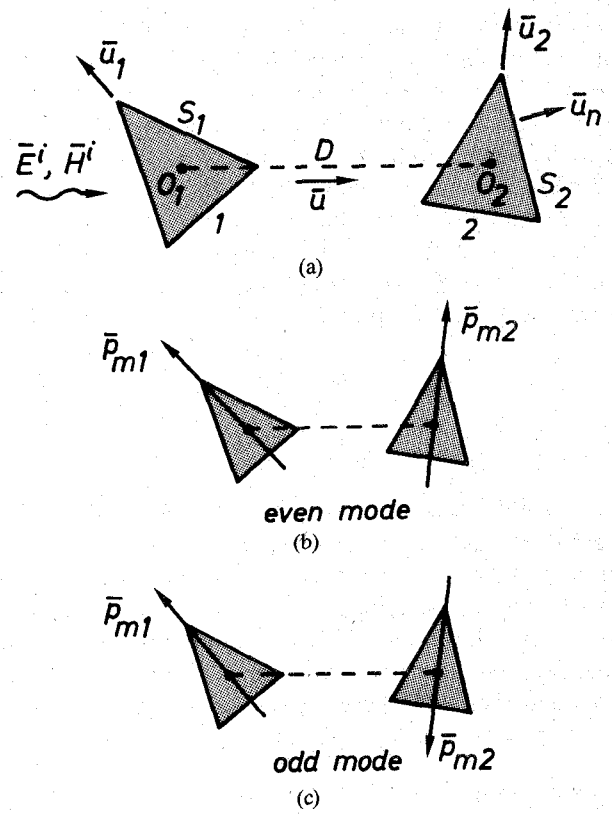

Fig. 1. Coupled resonators with corresponding resonant modes.

The conclusion is clear: the three-dimensional problem must be solved. To avoid this very arduous task, approximations have been made in the past [3], [4]. Cohn, for example, represents dielectric resonators by conducting loops carrying currents I, and endowed with L, C, and

0018-9480/82/1100-1907$00.75 ©1982 IEEE